

# Water-Triggered Photoinduced Electron Transfer in Acetonitrile-Water Binary Solvent. Solvent Microstructure-Tuned Reactivity of Hydrophobic Solutes

*Anna Lewandowska-Andralojc<sup>\*a,b</sup>, Gordon L. Hug<sup>c</sup>, Bronislaw Marciniak<sup>a,b</sup>, Gerald Hörner<sup>d</sup>,  
Dorota Swiatla-Wojcik<sup>\*e</sup>*

<sup>a</sup>Faculty of Chemistry, Adam Mickiewicz University, Uniwersytetu Poznanskiego 8, 61-614,  
Poznan, Poland, [alewand@amu.edu.pl](mailto:alewand@amu.edu.pl)

<sup>b</sup>Center for Advanced Technology, Adam Mickiewicz University, Uniwersytetu  
Poznanskiego 10, 61-614 Poznan, Poland

<sup>c</sup>Radiation Laboratory, University of Notre Dame, Notre Dame, USA

<sup>d</sup>Institut für Anorganische Chemie IV, Universität Bayreuth Universitätsstraße 30, NW I,  
95540 Bayreuth, Germany

<sup>e</sup>Institute of Applied Radiation Chemistry, Faculty of Chemistry, Lodz University of  
Technology, Zeromskiego 116, 90-924 Lodz, Poland

[swiatlad@p.lodz.pl](mailto:swiatlad@p.lodz.pl)

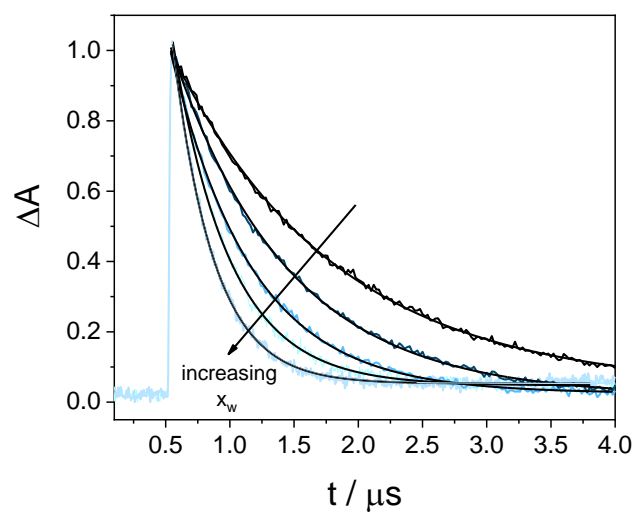


Figure S1. Normalized decay profiles at 520 nm obtained during laser flash photolysis at 355 nm of deoxygenated solutions of benzophenone ( $2.5 \times 10^{-3}$  M) and anisole (0.006 M) in different ACN-H<sub>2</sub>O mixtures ( $x_w$  from 0.34 to 0.81).

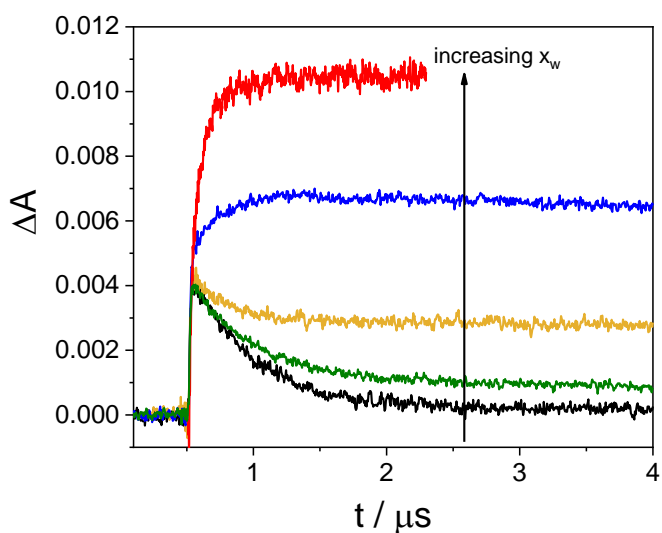


Figure S2. Decay profiles at 600 nm obtained during laser flash photolysis at 355 nm of deoxygenated solutions of benzophenone ( $2.5 \times 10^{-3}$  M) and anisole (concentration for 90% of quenching) in different ACN-H<sub>2</sub>O mixtures,  $x_w = 0.66$  black symbols;  $x_w = 0.74$  green symbols;  $x_w = 0.81$  yellow symbols;  $x_w = 0.89$  blue symbols;  $x_w = 0.92$  red symbols.

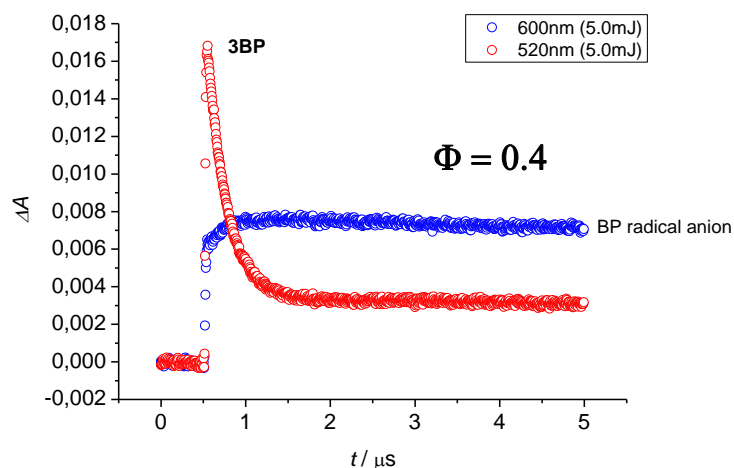


Figure S3. Decay profiles obtained during laser flash photolysis at 355 nm of deoxygenated solutions of benzophenone ( $2.5 \times 10^{-3}$  M) and anisole ( $4.6 \times 10^{-3}$  M anisole) in ACN-H<sub>2</sub>O (1:4 v/v), (520 nm (red), 600 nm (blue)).

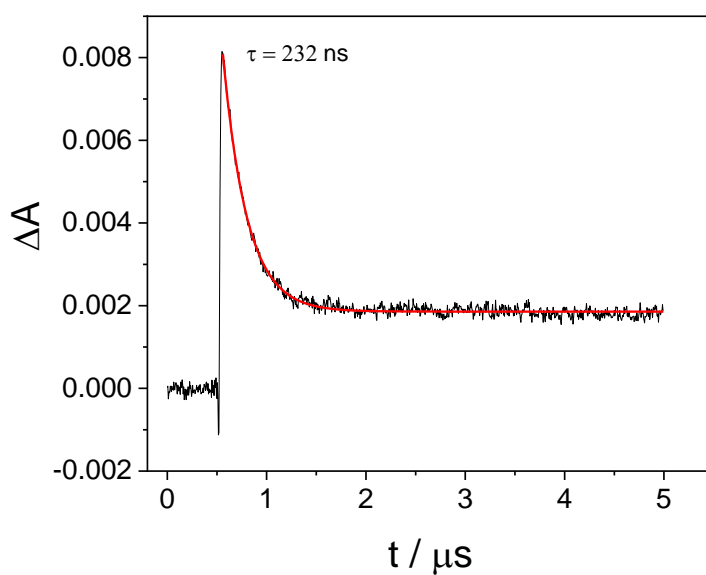


Figure S4. Decay profiles at 480 nm obtained during laser flash photolysis at 355 nm of deoxygenated solutions of benzophenone ( $2.5 \times 10^{-3}$  M) and anisole ( $4.6 \times 10^{-3}$  M anisole) in ACN-H<sub>2</sub>O (1:4 v/v). Solid curve is the monoexponential fit, the number represents the value obtained from the fit to kinetic profile.

## Collins-Kimball model adopted for rationalization of kinetics model

The estimates of the following are based on the Collins-Kimball solution to contact diffusion-reactions with  $u(r) = 0$ , adopted from literature [1]:

$$k(t) = k \left[ 1 + \frac{k_0}{k_D} e^{\alpha^2 t} \operatorname{erfc}(\alpha \sqrt{t}) \right] = \begin{matrix} k_0 & \text{at} & t = 0 \\ k & \text{at} & t = \infty \end{matrix} \quad (\text{Eq. S1})$$

$$k_D = 4\pi\sigma D \quad (\text{Eq. S2})$$

$$\alpha = \sqrt{\frac{D}{\sigma^2} \left[ 1 + \frac{k_0}{k_D} \right]} \quad (\text{Eq. S3})$$

$$k = \frac{k_0 k_D}{k_0 + k_D} \quad (\text{Eq. S4})$$

or

$$\frac{1}{k} = \frac{1}{k_0} + \frac{1}{k_D} \quad (\text{Eq. S5})$$

At 25 °C the diffusion constants of acetonitrile and water are  $3.18 \times 10^{-5} \text{ cm}^2\text{s}^{-1}$  and about  $2 \times 10^{-5} \text{ cm}^2\text{s}^{-1}$ , respectively. Putting these diffusion constants into the equation for  $\alpha$  along with  $\sigma$  of the order of 7 Å and  $\frac{k_0}{k_D}$  the order of 1 or smaller, the factor  $e^{\alpha^2 t} \operatorname{erfc}(\alpha \sqrt{t})$  goes to zero very rapidly with time. This is illustrated in the simulation presented in Figure S5.

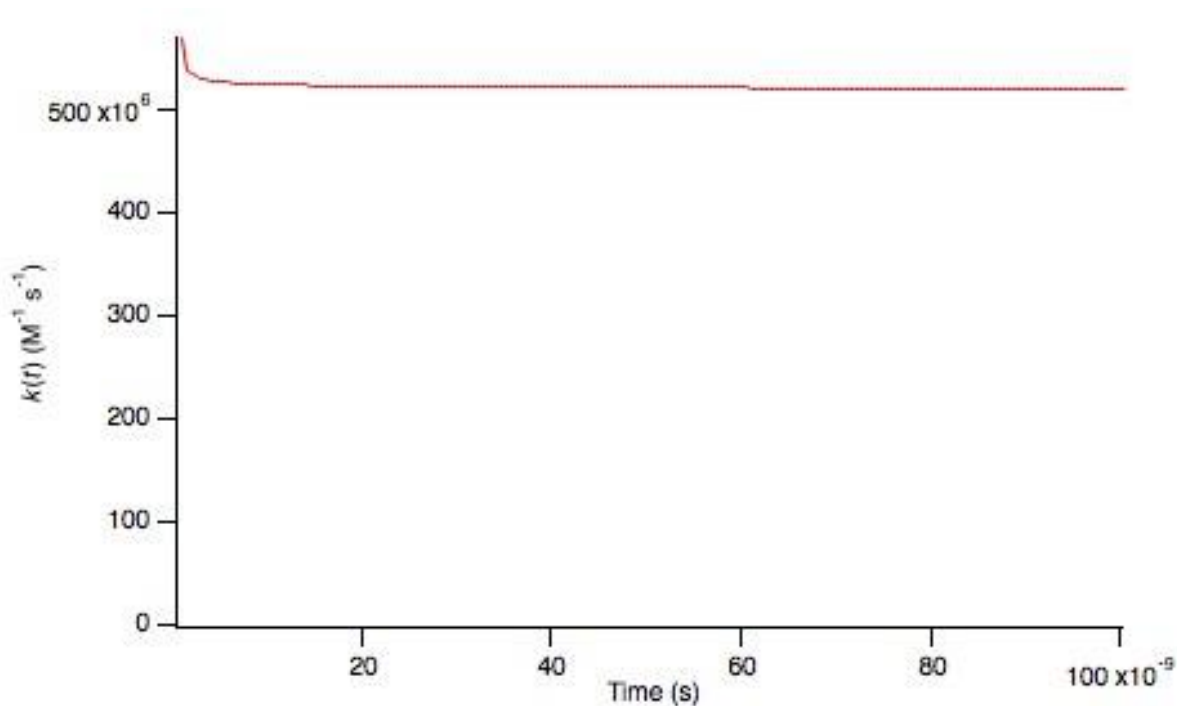


Figure S5. Collins-Kimball solution to diffusion quenching in free space.

The contact reaction rate constant was chosen  $k_0 = 5.96 \times 10^8 \text{ M}^{-1} \text{ s}^{-1}$  to be consistent with the steady-state equation,  $\frac{1}{k} = \frac{1}{k_0} + \frac{1}{k_D}$ , using  $k = 5.4 \times 10^8 \text{ M}^{-1} \text{ s}^{-1}$  which is the largest empirical  $k_q$  (plotting  $k(\text{obs})$  vs  $[Q]$ ) measured at  $\chi_w = 0.92$ .  $k_D$  was taken to be  $5.79 \times 10^9 \text{ M}^{-1} \text{ s}^{-1}$  (using the viscosity interpolated to the value at  $\chi_w = 0.92$  from ref. [2]) in computing  $k_0$  used in the Figure S5. In particular, we computed  $\frac{1}{k_0} = \frac{1}{k_q} - \frac{1}{k_D}$ . This simulation shows that on the time scale used in the experiments performed in this study, namely measuring triplet quenching, it is not expected to see the transient in a time-dependent quenching rate constant. Single exponential decays were observed in all of kinetic traces, and, empirically, all pseudo-first order plots, namely dependence of reciprocal lifetimes vs quencher concentration were linear.

In addition, in Burshtein's "kinetic limit"[1], the generally time-dependent rate constant,  $k(t)$ , becomes a time-independent rate constant,  $k_0$ . In the Figure S5, the time-dependent Collins-

Kimball rate constant reaches a plateau as it just gets into the nanosecond range. In summary, the steady-state Collins-Kimball solution

$$\frac{1}{k_q} = \frac{1}{k_0} + \frac{1}{k_D} \quad (\text{Eq. S6})$$

can be used for the analysis of the second-order quenching rate,  $k_q$ .

### **Rational for viscosity not accounting for the observations**

Viscosity considered as the sole factor for our observed variation in  $k_q$  cannot account for the quantitative behavior of the empirical quenching rate constant as a function of solvent composition in this case. Viscosity ( $\eta$ ) would come into the equation for  $k_q$  as  $k_D = k_B T / (6\pi\eta\sigma)$ . This cannot explain the change in  $k_q$  from  $4.6 \times 10^6 \text{ M}^{-1} \text{ s}^{-1}$  at  $\chi_w = 0$  to  $5.4 \times 10^8 \text{ M}^{-1} \text{ s}^{-1}$  at  $\chi_w = 0.92$  (a change in quenching rate constant by factor of 100) because the viscosity at the extremes changes only by a factor of 0.38 mPa s to 1.1 mPa s going from  $\chi_w = 0$  to  $\chi_w = 0.92$ [2]. Because of the relationship between diffusion constant and viscosity being reciprocal, this relationship is even in the wrong direction for viscosity to account for our observations.

### **Continuous solvent model in the Marcus-theory**

The values for the squared refractive index ( $n_D^2$ ) and the static dielectric constant ( $\epsilon_s$ ) for the ACN-water mixtures where extrapolated from the refs. [2-4] and plotted in Figure S6 and Figure S7, respectively.

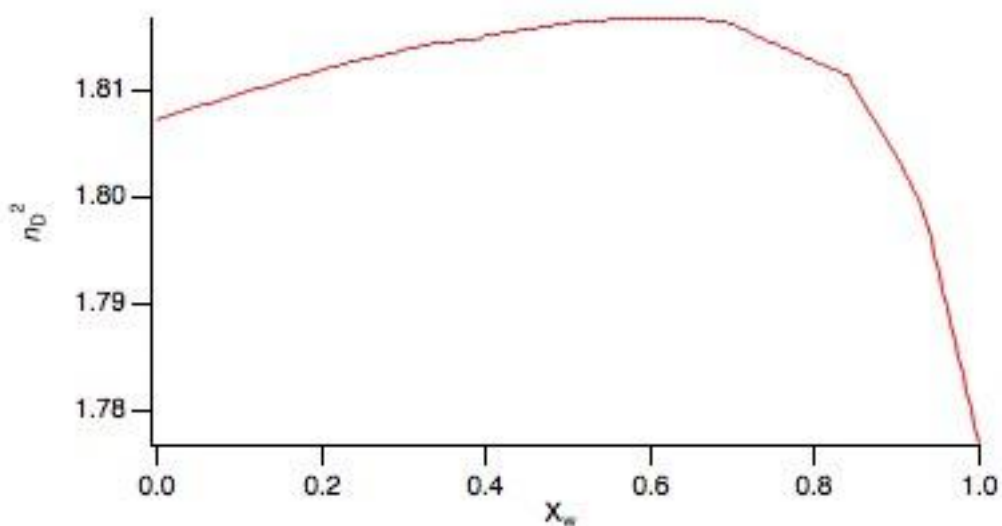


Figure S6. Squared refractive indexes as a function mole fraction of water interpolated from the refs. [2, 4].

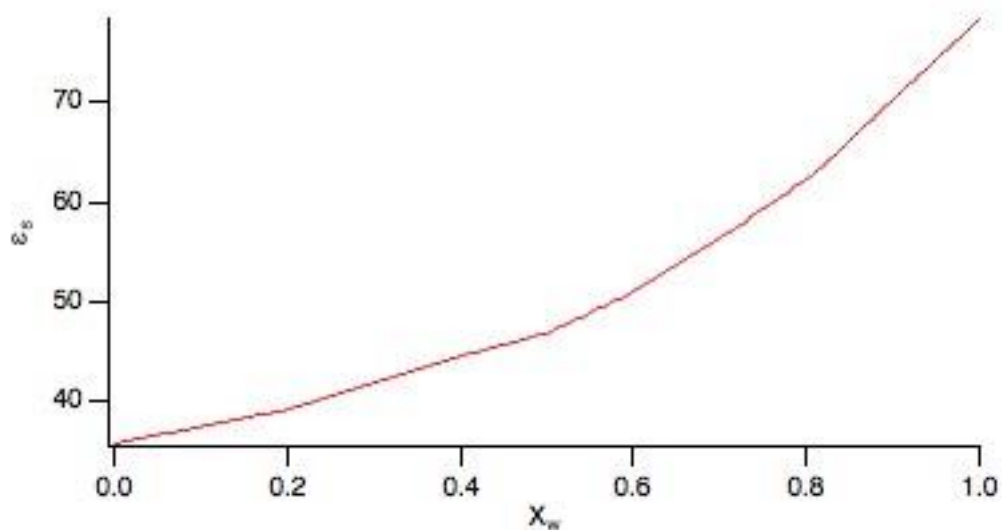


Figure S7. Interpolated static dielectric constants as a function of  $x_w$  from the ref. [3]

Based on the data plotted on Figure S6 and Figure S7 solvent reorganization energies for various ACN-H<sub>2</sub>O mixtures were calculated using the Born formula for the free energies of ions in solution:

$$\lambda = e^2 \left( \frac{1}{2r_B} + \frac{1}{2r_Q} - \frac{1}{r_{BQ}} \right) \left( \frac{1}{n_D^2} - \frac{1}{\epsilon_s} \right) \quad (\text{Eq. S7})$$

Where:  $r_B$  – is the radius of the BP anion ( $3.5 \times 10^{-8}$  cm),  $r_Q$  – is the radius of anisole cation ( $3.5 \times 10^{-8}$  cm) and  $r_{BQ}$  – is center-to-center separation of radical ions at contact ( $7 \times 10^{-8}$  cm). The dependence of the solvent reorganization energies on the ACN-H<sub>2</sub>O mixture composition is depicted in Figure S8.

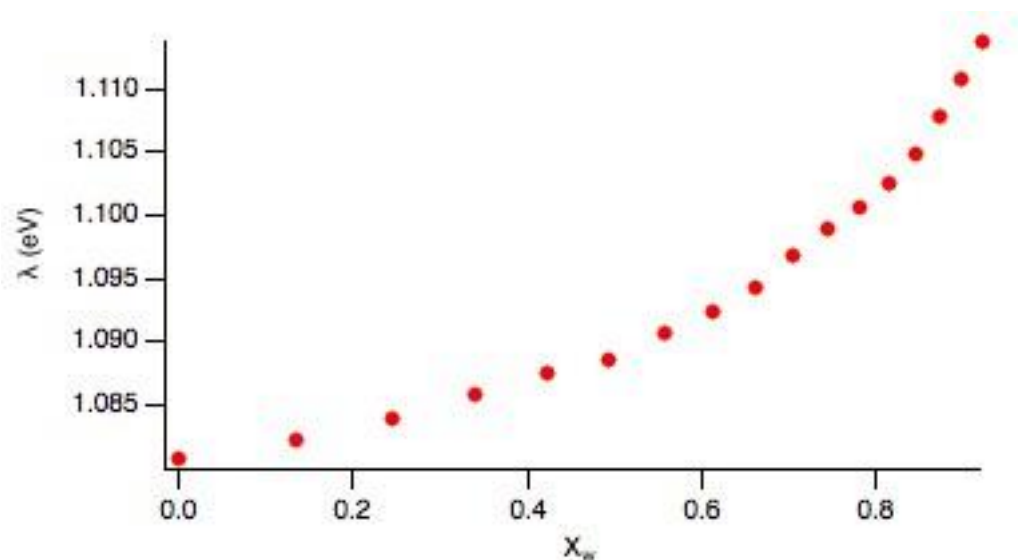


Figure S8. Solvent reorganization energies as function of  $x_w$  calculated using the Born formula (Eq. S7).

Subsequently, the  $\Delta G_{ET}^0$  for electron transfer process was computed based on the Eq. S8:

$$(\Delta G_{ET}^0)_{\chi w} = (E_{ox} - E_{red})_{\chi w} - \frac{e^2}{(\epsilon_s)_{\chi w} r_{BQ}} - E_T \quad (Eq. S8)$$

Where:  $\frac{e^2}{(\epsilon_s)_{\chi w} r_{BQ}}$  is the energy of interaction of the radical ions at contact,  $E_T$  is the benzophenone triplet energy (3.0 eV),  $(E_{ox} - E_{red})_{\chi w}$  is the value taken from ref. [5] equal 3.59 eV for pure ACN and 3.29 eV for all other molar fractions.

In the next step, Marcus activation energy was computed according to Eq. S9

$$E_A = \frac{(\Delta G_{ET}^0 + \lambda)^2}{4\lambda} \quad (Eq. S9)$$



Finally, the rate constants as a function of water mole fractions based on the classical Marcus theory was computed from Eq. S10 and plotted in Figure S9

$$k_{ET} = \frac{2\pi}{\hbar} V_{BQ}^2 \frac{1}{\sqrt{4\pi\lambda k_B T}} \exp\left(-\frac{E_A}{k_B T}\right) \quad (\text{Eq. S10})$$

Where:  $V_{BQ}$  – is the exchange interaction at contact between excited B and Q (0.01 eV)

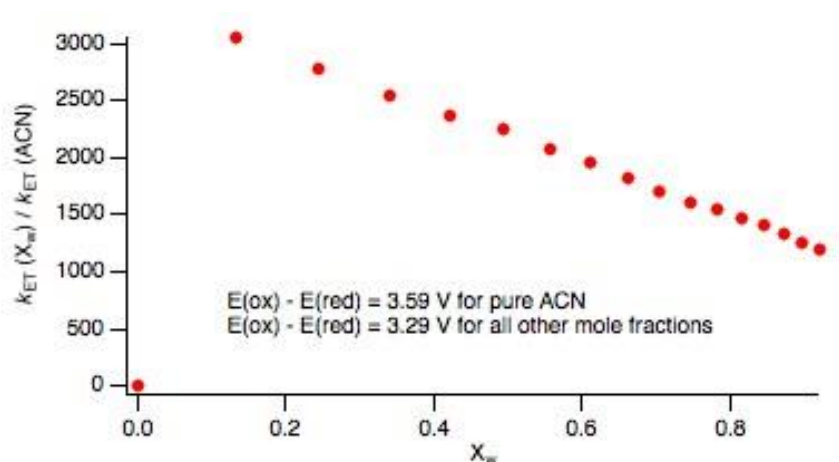


Figure S9. Ratio of the classical rate constant for electron transfer for various ACN-H<sub>2</sub>O mixtures to rate constant for electron transfer in ACN as a function of  $x_w$  calculated from Marcus theory (Eq. S10).

Figure S9 shows that using continuum-solvent model as a function of refractive index, static dielectric constant and hydrogen bonding interactions that affect the  $(E_{ox} - E_{red})$  one obtains the variation of electron-transfer rate constants that doesn't match our experimental data.

## References

- [1] A. I. Burshtein, *Adv. Chem. Phys.*, **2004**, *129*, 105-418.
- [2] A.-L. Vierk, *Z. Anorg. Chem.*, **1950**, *261*, 283-296.
- [3] R. Jellema, J. Bulthuis, G. van der Zwan, *J. Mol. Liq.*, **1997**, *73-74*, 179-193.
- [4] J. E. Bertie, Z. Lan, *J. Phys. Chem. B*, **1997**, *101*, 4111-4119.
- [5] A. Lewandowska, G. L. Hug, G. Hörner, T. Pedzinski, P. Filipiak, B. Marciniak, *ChemPhysChem*, **2010**, *11*, 2108-2117.